BOREAL ENVIRONMENT RESEARCH 18: 89–108
ISSN 1239-6095 (print) ISSN 1797-2469 (online)

Helsinki 5 April 2013

Seasonal and annual heat budgets offshore the Hanko Peninsula, Gulf of Finland

Ioanna Merkouriadi[1)]*, Matti Leppäranta[1)] and Kunio Shirasawa[2)]

[1)] *Department of Physics, P.O. Box 48, FI-00014 University of Helsinki, Finland (*corresponding author's e-mail: ioanna.merkouriadi@helsinki.fi)*
[2)] *Pan-Okhotsk Research Center (P-ORC), Institute of Low Temperature Science Hokkaido University, Kita-19, Nishi-8, Kita-Ku, Sapporo 060-0819 Japan*

Received 4 Oct. 2011, final version received 20 June 2012, accepted 29 Mar. 2012

Merkouriadi, I., Leppäranta, M. & Shirasawa, K. 2013: Seasonal and annual heat budgets offshore the Hanko Peninsula, Gulf of Finland. *Boreal Env. Res.* 18: 89–108.

A joint Finnish–Japanese sea-ice experiment "Hanko-9012" carried out offshore the Hanko Peninsula included seasonal monitoring and intensive field campaigns. Ice, oceanographic and meteorological data were collected to examine the structure and properties of the Baltic Sea brackish ice, heat budget and solar radiation transfer through the ice cover. Here, the data from two years (2000 and 2001) are used for the estimation of the seasonal and annual heat budgets. Results present the surface heat balance, and the heat budget of the ice sheet and the waterbody. The ice cover acted as a good control measure of the net surface heat exchange. Solar radiation had a strong seasonal cycle with a monthly maximum at 160 and a minimum below 10 W m^{-2}, while net terrestrial radiation was mostly between –40 and –60 W m^{-2}. Latent heat exchange was much more important than sensible heat exchange, similar the net terrestrial radiation values in summer and autumn. A comparison between the latent heat flux released or absorbed by the ice and the net surface heat fluxes showed similar patterns, with a clearly better fit in 2001. The differences can be partly explained by the oceanic heat flux to the lower ice boundary.

Introduction

The Hanko Peninsula is located on the southwest Finnish coast, at the mouth of the Gulf of Finland in the Baltic Sea. Each winter, landfast ice forms along the Finnish coast of the Gulf of Finland. Ice starts to form in December and melts away in April. The thickness of the ice varies significantly among seasons, reaching up to 80 cm (Seinä and Peltola 1991). The formation of ice has significant effects on both the physics and the ecology of the Gulf of Finland. The inner archipelago at the Hanko Peninsula is ice-covered every winter, and in three out of four winters the brackish waters further offshore freeze over. There the maximum annual thickness can reach up to 50 cm, and the ice sheet consists mostly of congelation ice and snow-ice.

Santala Bay, located at the northwest coast of the Hanko Peninsula, was the main research site of the "Hanko-9012" experiment in 1999–2002 (Granskog *et al*. 2004). Each year, there was an all-season monitoring program, and intensive field study phases were performed a few times. The purpose of the experiment was to examine the structure and properties of the Baltic

Editor in charge of this article: Kai Myrberg

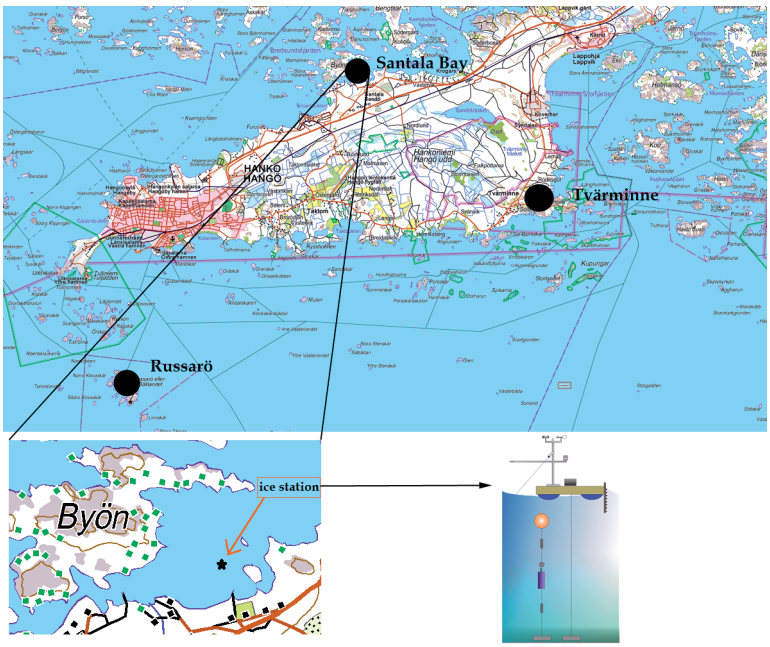

Fig. 1. The Hanko Peninsula with the Santala site, Tvärminne Zoological Station and Russarö Weather Station (top) [map courtesy of the National Land Survey of Finland]; and Santala Bay and the schematic profile of the automatic station (bottom).

brackish ice, heat budget, solar radiation and ice–brackish-water interaction. The region also provided an opportunity to examine the transition zone between fresh water ice and sea ice (Kawamura *et al*. 2002).

In the coastal zone, the annual variability of the heat budget is large, with ice in winters and surface temperatures exceeding 20 °C in summers. Sea ice growth and decay is forced by the heat fluxes through its upper and lower boundaries. Due to the scarcity of continuous, good observation records, examination of sea ice thermodynamics has been mainly approached by mathematical modelling. The data obtained from the "Hanko-9012" experiment, cover the seasons from autumn to spring. To add the summer period, additional atmospheric and water-temperature data from the Russarö Weather Station and the Tvärminne Zoological Station were used. Together, these data allowed us to estimate the annual course of the heat budget.

The purpose of this work was to compute the heat flux components between the surface and the atmospheric boundary layer (ABL) throughout the year. In addition to that, we focused on the ice mass and heat budget in winter together with the changes in the heat content of the ice and waterbody. This is the first study of the annual course of the heat budget in the Baltic Sea based purely on observations, including the ice season.

Material and methods

The study site

The experiment site was Santala Bay (59°55´N, 23°05´E), located at the northwest coast of the Hanko Peninsula, on the southern part of the Finnish coast. The bay communicates with the Gulf of Finland through a southwest passage and with the inner archipelago through a wider opening northeast (Fig. 1).

A floating platform, which was designed and built in 1998, was positioned at the study site in Santala Bay for four ice seasons, 1999–2002 (Fig. 1). The depth of the sea at the site was 10 m. The platform consisted of a wooden deck (2 × 2 m) and four polyurethane floats covered by thick plastic. It was located in the center of Santala Bay, anchored with four anchors, one from each side. One lighter weight was attached under the platform in order to keep it steady in the presence of wind-driven surface waves. Each year after the melting of sea ice, the platform

was recovered and stored during the summer season.

Data

The first winter (1999) was a pilot study and the data were collected only in March, while during the last winter, there were some data acquisition problems. Therefore, this work is focused on two years, 2000 and 2001 (Table 1). The instrumentation of the station (Grant Instruments, UK) included atmospheric, ice and water sensors. The sampling interval was 1 hour. The measured parameters (Tables 2 and 3) were:

- Atmospheric surface layer: temperature, humidity, wind speed and direction, incoming and outgoing solar radiation, and surface radiative temperature.
- Water: temperature, salinity and three-dimensional water flow in one fixed depth (5 m).
- Ice: temperature profile, thickness and Photosynthetically Active Radiation (PAR).

In addition to the automatic recordings, the site was visited once a week. The ice and snow were sampled weekly for thickness and stratification. The ice sheet consisted of an upper snow-ice layer, formed from frozen slush, and a lower congelation ice layer, formed from sea water at the bottom of the sea ice (Weeks 1998). In mid-winter, there was usually snow on the ice. Analysis of the ice structure in Santala has been presented by Kawamura *et al*. (2001).

The Santala automatic station was recording continuously over the ice season for 6–7 months during each year (Table 1). In order to estimate the annual heat fluxes, the missing data for the summer period were obtained from the Tvärminne Zoological Station located on the southwest coast of the Hanko Peninsula, and the Russarö Weather Station located on Russarö, an island some 3 km south from the Peninsula (Fig. 1).

On the premises of the Tvärminne Zoological Station there is a simple weather station belonging to the Finnish Meteorological Institute (FMI) which measures air temperature (at 2 m), relative humidity (at 2 m) and precipitation which is recorded during three periods of the day (06:00–12:00, 12:00–18:00, and 18:00–06:00), and the dataset contains information about:

- the amount of precipitation (in mm of liquid water) during the 3-day periods and
- the precipitation types (solid/liquid) by using the international code system.

Table 1. Data collection during the 2000 and 2001 winters.

Season	Intensive phase	Automatic station
1999–2000	15–31 Mar	15 Dec–27 Jun
2000–2001	–	13 Dec–7 May

Table 2. Sensors and their positions in the years 1999–2000.

Automatic station/sensor	Height (cm)	Start time (date, UTC)	End time (date, UTC)
Platform			
Wind speed	120, 215	15 Dec. 1999, 13:00	27 June 2000, 18:00
Wind direction	215		
Surface radiative temperature	0		
Air temperature	95, 198		
Relative humidity	95		
Incoming solar radiation (PAR and broadband)	100, 198		
Outgoing solar radiation (broadband)	96		
Thermistor strings			
Ice-water temperature	0, 20, 40, 60		
Air–ice–water temperature	–10, –5, 0, 5, 10, 15, 20, 30		

The sea-surface temperature, which is critically important for the closure of the open water surface heat balance, is measured daily by the staff of the Tvärminne Zoological Station. The Russarö Meteorological Station provided the wind speed and cloudiness data. The wind speed data from Russarö were used after modification (*see* Data analysis).

Data analysis

The heat flux between the sea surface and the atmospheric boundary layer is determined by solar radiation (Q_{sc}), terrestrial radiation (Q_L), turbulent heat fluxes (Q_H and Q_e) and heat flux from precipitation (Q_P). Each component was calculated for the years 2000 and 2001 with a 3-hour time step.

Net solar radiation

The difference between the incoming and the outgoing solar radiation gives the net solar radiation flux. The incoming radiation (Q_s) can be either measured directly or estimated using the following formula (Iqbal 1983):

$$Q_s = \cos Z T_{tr}(Z,e) F(N,Z)(r_0/r)^2 Q_{sc} \qquad (1)$$

where Z is the solar zenith angle, T_{tr} is the atmospheric clear-sky transmissivity, e is the atmospheric water-vapor pressure, F is the fraction that indicates the effect of cloudiness N ($0 \le N \le 1$), r and r_0 are the actual and average Earth–Sun distances, respectively, and Q_{sc} = 1.376 kW m^{-2} is the solar constant. The transmissivity and cloudiness corrections were taken from Zillman (1972: 413–444) and Lumb (1963), respectively.

While the automatic station was operating, the solar radiation was measured directly. In the year 2000, pyranometers were used to measure the broadband solar irradiance (incoming and outgoing). In 2001, only the outgoing irradiance was available from one pyranometer. The incoming irradiance was estimated using a quantum PAR (Photosynthetically Active Radiation) sensor. This sensor calculates the number of photons per unit area and time, and a constant I/E ratio of 4.5 μmol s^{-1} W^{-1} was used (Reinart and Arst 1998) to convert to power units; here, I is the PAR quantum irradiance and E the PAR irradiance power. Measured outgoing irradiance and observed albedo values (Ehn *et al*. 2004, Arst *et al*. 2006) from Santala Bay were used to calibrate the PAR values and fit them to represent the broadband solar radiation spectrum.

Net terrestrial radiation

The net terrestrial (longwave) radiation is the difference between the thermal radiation emitted by the atmosphere and the thermal radiation emitted by the sea surface. The latter represents the energy loss term and is given by the grey-body law:

Table 3. Sensors and their positions in the years 2000–2001.

Automatic station/sensor	Height (cm)	Start time (date, UTC)	End time (date, UTC)
Platform			
Wind speed	117, 215	13 Dec. 2000, 14:00	7 May 2001, 08:00
Wind direction	215		
Surface radiative temperature	0		
Air temperature	95, 195		
Relative humidity	95		
Incoming solar radiation (PAR)	200		
Outgoing solar radiation (broadband)	96		
Ice-water temperature	0, 10, 20, 40, 60, 80		
Air-ice-water temperature	–10, –5, 0, 5, 10, 15, 20, 30		

Note: 0 cm height values correspond to initial water level height (without ice coverage).

$$Q_{L_0} = \varepsilon\sigma T_0^4 \quad (2)$$

where ε is the water/ice/snow emissivity, equal to 0.99 for water and 0.97 for ice/snow (Saloranta 2000), σ = 5.67 10^{-8} W m^{-2} K^{-4} is the Stefan–Boltzmann constant, and T_0 is the absolute surface temperature in Kelvin.

The thermal radiation emitted by the atmosphere is a more complicated term, since it is generated by atmospheric water droplets, aerosols and gas molecules at different heights and temperatures. In calculations, the following equations based on the grey-body formula were used:

$$Q_{L_a} = \varepsilon_a\sigma T_a^4 \quad (3)$$
$$\varepsilon_a = \varepsilon_a(N,e) = (a + be^{1/2})(1 + cN^2) \quad (4)$$

where ε_a is the effective atmospheric emissivity; a, b and c are constants equal to 0.68, 0.036 mbar$^{-1/2}$ and 0.18, respectively (e.g. Omstedt 1990).

Turbulent heat fluxes

The turbulent heat exchange between the sea surface and the atmosphere is described by the sensible and latent heat fluxes. To estimate these fluxes, the bulk formulae were used (Leppäranta and Myrberg 2009):

$$Q_H = \rho_a c_p C_H (T_a - T_0) U_a \quad (5)$$
$$Q_e = \rho_a L_E C_E (q_a - q_0) U_a \quad (6)$$

where ρ_a and c_p are the density and specific heat of air, L_E is the enthalpy of evaporation equal to 2.5 W J kg^{-1}, q_0 and q_a are the specific humidities at the sea surface and in the atmosphere (at the reference level of 2 m), respectively, and U_a is the wind speed. The Stanton and the Dalton numbers, C_H and C_E, are the bulk transfer coefficients. In neutral atmospheric conditions, they are taken as constants normally varying between 1.0×10^{-3} and 1.5×10^{-3} (Andreas 1987). However, the atmospheric stratification above the sea-ice surface is not always neutral stability (Launiainen and Vihma 2001).

According to the Monin-Obukhov similarity law, the turbulent transfer coefficients are defined as (Garratt 1992):

$$C_h = \kappa^2 \left(\ln\frac{z}{z_0} - \Psi_M\frac{z}{L} \right)^{-1} \left(\ln\frac{z}{z_t} - \Psi_h\frac{z}{L} \right)^{-1} \quad (7)$$

$$C_e = \kappa^2 \left(\ln\frac{z}{z_0} - \Psi_M\frac{z}{L} \right)^{-1} \left(\ln\frac{z}{z_q} - \Psi_h\frac{z}{L} \right)^{-1} \quad (8)$$

where κ is the von Karman constant ($\approx$ 0.4), Ψ_M, Ψ_h and Ψ_e are the universal functions which characterize the effect of the atmospheric surface layer stability on the bulk transfer coefficients; $z/L = \zeta$ is the non dimensional stability parameter based on the Obukhov length L (Obukhov 1981) which is given by

$$L = -u_*^3 \overline{T} \rho_a c_p \left[g\kappa Q_h \left(1 + \frac{0.61\overline{T}c_p Q_e}{Q_h L_e} \right) \right]^{-1} \quad (9)$$

where u_* is the friction velocity, g the gravity acceleration and $\overline{T} = (T_0 + T_s)/2$. In case of neutral or stable stratification ($\zeta \geq 0$), we used the forms of Holtslag and De Bruin (1988). In unstable conditions ($\zeta < 0$), we used the forms of Högström (1988). There is, however, a numerical problem since z_0 and u_* cannot be obtained simultaneously. This was solved by applying an iteration routine suggested by Launiainen and Saarinen (1982) and Launiainen and Vihma (1990).

When the automatic station was operating, we estimated the correlation between the wind speed data from Santala (U_S) and Russarö (U_R) at reference heights of 2 m and 10 m, respectively. The correlation coefficient varied between 0.8 and 0.85. A fairly good estimation of the wind speed in Santala Bay is given by the linear expression $U_S = 0.65U_R$.

Precipitation

Precipitation is a heat exchange mechanism acting both as sensible heat and as phase changes. It is not often included in the heat budget analysis. However, in the case of phase changes it can be an important heat transfer mechanism. This heat flux can be expressed as (Leppäranta and Myrberg 2009):

$$Q_p = \rho[c(T_P - T_0) + L_f\chi_P]P \quad (10)$$

where ρ and c are the density and heat capacity in precipitating medium (liquid water or ice),

$\chi_P = -1, 0$, or 1 for solid to liquid phase change, no phase change, or liquid to solid phase change, respectively, L_f is the latent heat of freezing (335 kJ kg^{-1}), T_P and T_0 are the temperatures of precipitation and sea surface, respectively, and P is the precipitation. The dominant term is the phase change. Sensible heat transfer with precipitation was ignored in the present work.

Oceanic heat flux from water to ice

After evaluating the heat exchange in the ABL, we attempted to close the ice–water-column system by monitoring the sea-ice growth and decay. The surface heat flux is balanced by the oceanic heat flux and change in the ice thickness. The oceanic heat flux, acting on the bottom of the sea ice, is still a not well-known quantity, in the present case anticipated to be of the order of 10 W m^{-2} (Shirasawa *et al*. 2006).

An indirect way to estimate the oceanic heat flux to the ice is to take the residual (Leppäranta and Myrberg 2009):

$$Q_w = \kappa_i \frac{\partial T}{\partial z} - \rho L \frac{dh}{dt} \qquad (11)$$

where κ_i = 2.1 W m^{-1} °C^{-1} is the thermal conductivity of the ice, ρ is the ice density, and h is the ice thickness. The first term on the right-hand side represents the conductive heat flux to the ice layer, and the second one the heat released/used during the ice growth/melting. Since the ice is rather thin at the site, we could approximate the heat conduction from ice bottom to be equal to the air–ice heat transfer, and then oceanic heat flux becomes the balancing residual.

Advection of heat from the central gulf

The mean temperatures of the water and ice thickness give the heat content of the ice–water system. Oceanic heat flux is an internal process there. Changes of the heat content are forced by the surface heat flux and advection from the central gulf. Since here we were measuring the surface heat fluxes and changes in the heat content of the ice–water system, advection becomes a residual.

Accuracy of the heat budget

In general, the accuracy of the heat budget components is good, especially over the winter and spring seasons when the float was operating. Occasionally, there might be short-term problems but considering the monthly balances errors are largely compensated. The most uncertain term is the net terrestrial radiation, since the atmospheric radiation was estimated based on cloudiness in Russarö. The sensitivity of atmospheric emissivity to cloudiness is

$$\frac{\delta\varepsilon_a}{\varepsilon_a} = \frac{2cN\delta N}{(1+cN)} \approx 0.2\delta N \text{ for } N \approx 0.5,$$

which means that an error of 0.2 in cloudiness gives an error of 4% in the atmospheric radiation, equal to about 10 W m^{-2}. Because of the cloudiness difference between sea and land areas, the estimated atmospheric radiation may be biased down in summer and up in autumn and winter.

At the float, the net solar radiation was directly measured in 2000 while in 2001 it was estimated using the PAR measurements. The surface layer properties were also recorded properly to estimate the turbulent fluxes with also the stability of stratification accounted for. Over the summer when the float was inactive, there are additional inaccuracies due to estimating the solar radiation by an empirical formula and using the (calibrated) wind speed from Russarö for the turbulent fluxes. Then the cloudiness is the main problem for the solar radiation; the accuracy is proportional to $0.6\delta N/(1 - 0.6N)$. The accuracy of turbulent fluxes is proportional to the accuracy of the wind speed. Also, in the summer period the heat flux estimates are mainly based on Tvärminne data, located on the other side of the Hanko Peninsula at about 10 km from Santala.

Results

The net solar radiation flux

Solar radiation is the main heat source of the Earth system and it plays the primary role in the heating of the Baltic Sea. Due to the solar radiation flux, Baltic Sea ice starts melting in spring and the waterbody below gets warmer. In con-

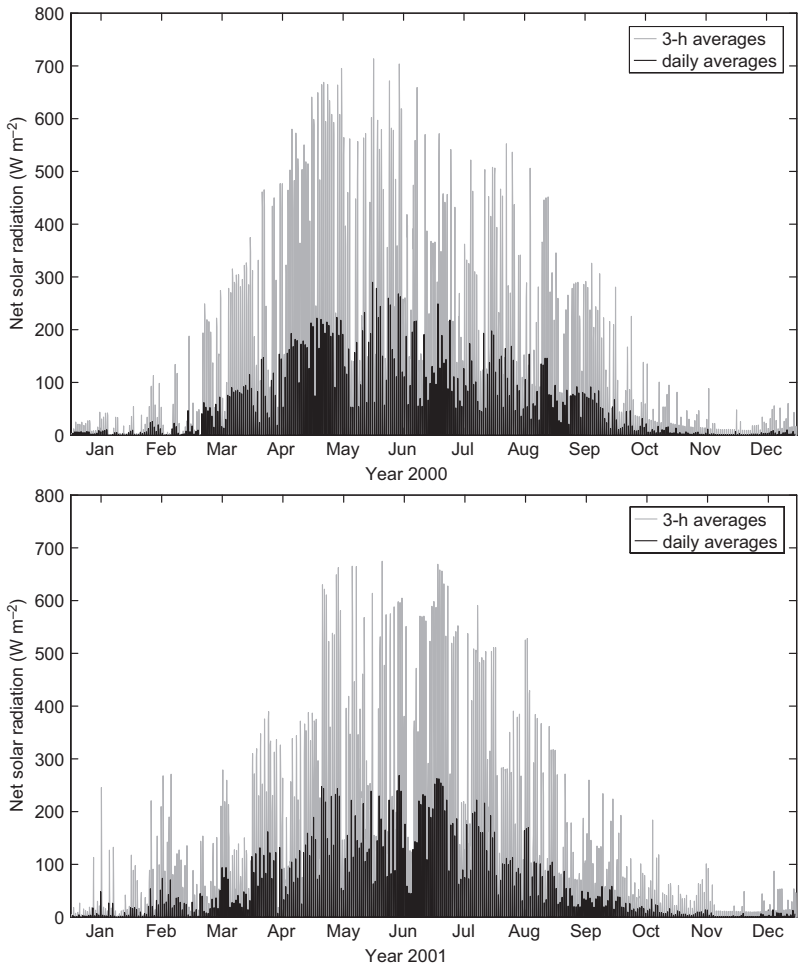

Fig. 2. Annual net solar heat flux in 2000 (top) and 2001 (bottom).

trast, during autumn and winter, thermal radiation and turbulent losses overcome solar radiation and this results in the cooling and freezing of the Baltic Sea water.

The amount of the net solar radiation was at the same level in both years (Fig. 2). In 2000 it was more intense during May, and in 2001 during July. Solar radiation is highly sensitive to cloudiness. In 2000 it was on average 67 W m^{-2} and the maximum was 705 W m^{-2}. As it was more intense in May, the average cloudiness was then less as compared with that in July. In 2001, solar radiation followed a similar pattern with an average of 66 W m^{-2} and a maximum of 673 W m^{-2}. In 2001, solar radiation reached higher values in July. Daily averages were above 200 W m^{-2} in summer and below 10 W m^{-2} in December–January (Fig. 2).

The net terrestrial radiation flux

Net terrestrial radiation was almost always negative since the atmospheric emissivity is much smaller than the surface emissivity (Fig. 3). It seems that the level was fairly stable throughout the year, around –50 W m^{-2}. The maximum daily mean was –9 W m^{-2} in 2000, and –3 W m^{-2} in 2001. The minimum daily mean was –90 W m^{-2} in 2000, and –121 W m^{-2} in 2001. The lowest values are due to high differences between the atmospheric and surface temperatures in clear sky conditions.

Turbulent heat fluxes

The average sensible heat flux was around

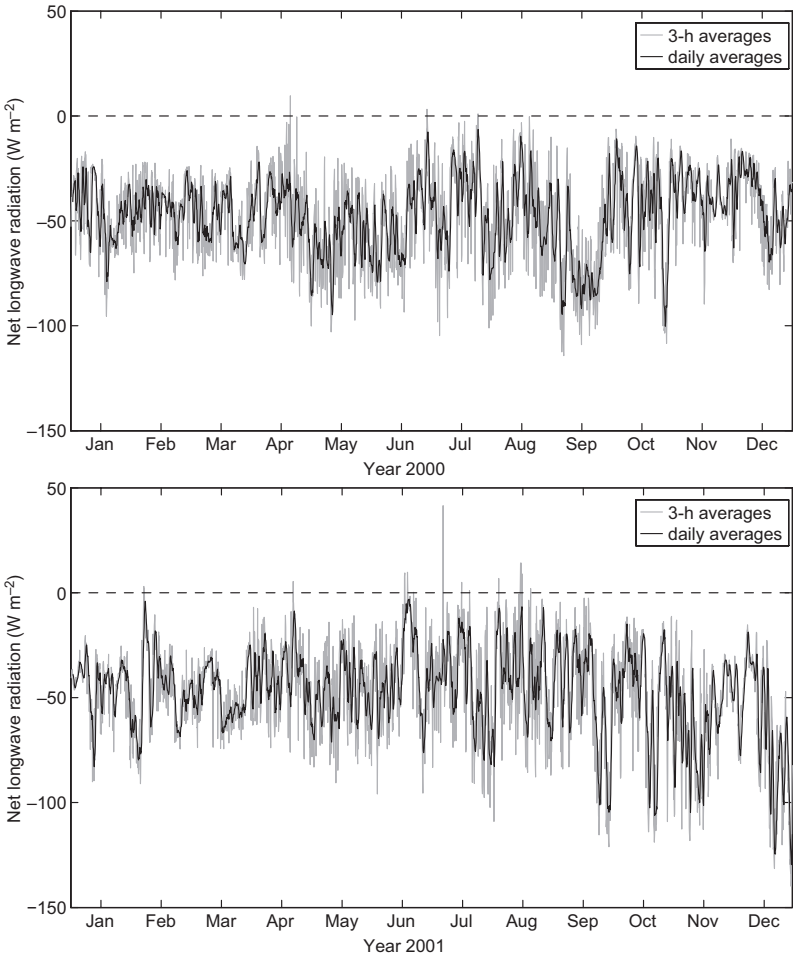

Fig. 3. Net terrestrial radiation flux in 2000 (top) and 2001 (bottom). The grey line represents the 3-hour averages and the black line daily averages.

–10 W m^{-2} in both years, similar to the daily averages. The lowest values occurred in autumn, especially in 2001, where a big drop occurred from November to December (Fig. 4).

The latent heat flux was almost always negative, with a daily mean of –30 W m^{-2} (Fig. 5). It appears that sensible heat fluxes were getting stronger in autumn, which is due to higher temperature differences between the surface and the atmosphere. The latent heat fluxes were stronger after the ice season and in autumn 2001. The monthly-average sensible heat fluxes were low in comparison with the other components. The latent heat fluxes have a higher influence on the heat budget and they were mainly negative except in extreme conditions. The average values were –30 W m^{-2} in both years and the minimum 3-hour value reached –203 W m^{-2} (corresponding to an evaporation of 1 mm/3 h) in 2001. The positive latent heat values, which were found a few times for winter, were due to sublimation on the ice surface.

Heat flux from precipitation

Positive values of heat exchange due to phase changes indicate liquid precipitation on ice surface, when the latent heat is released into the ice. This is why they only occur in the ice season (Fig. 6). Negative values indicate solid precipitation (snow) on open water surface when heat is released from the water for melting. These fluxes can be strong in short periods, but altogether, monthly averages were low ranging from –5 to 5 W m^{-2}. The highest monthly average

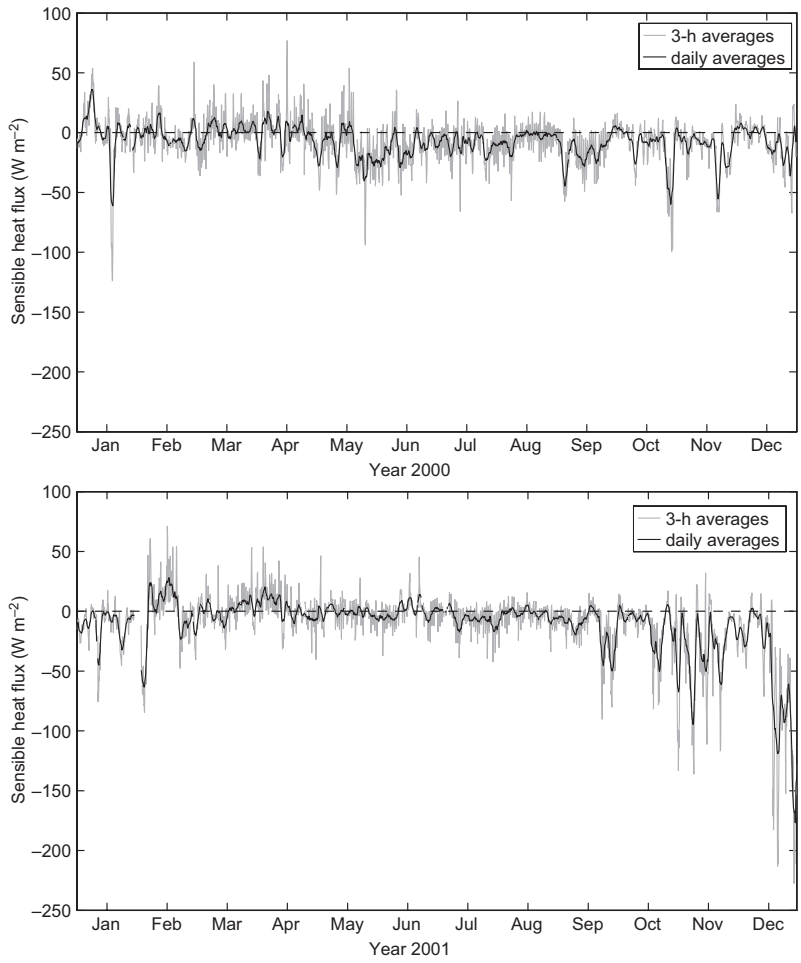

Fig. 4. Sensible heat fluxes in 2000 (top) and 2001 (bottom).

(–10 W m^{-2}) occurred in November 2001, meaning that there was a considerable amount of solid precipitation on the open water (Fig. 6).

Monthly averages of heat flux components

In general, patterns of the surface fluxes were similar in both years (Fig. 7, Tables 4 and 5). The main difference was in the turbulent heat fluxes in the autumn months (Fig. 7). In 2000, they were relatively small while in 2001 produced major heat losses. Thus, the quality of autumn cooling can differ much from year to year. Otherwise, it is clear that solar radiation is dominant throughout the year except the winter months. In the winter season, terrestrial radiation flux prevailed. In both years, the full balance was negative by about –20 W m^{-2} which resulted from fast cooling in the shallow archipelago in autumn. It is also considered that the autumn circulation was formed by the exchange of water between the cold coastal zone and the warm central gulf.

The terrestrial heat flux during the ice season was strongly negative (Fig. 8). The net solar radiation is limited in January and February and it increases fast towards May. The total surface heat flux was balanced during the ice season by latent heat released/used in ice growth/melting and oceanic heat flux from the Santala Bay waterbody through the ice.

The heat component values (Tables 4–7) are reasonable, resulting in a negative net annual heat flux in both years (~ –20 W m^{-2}).

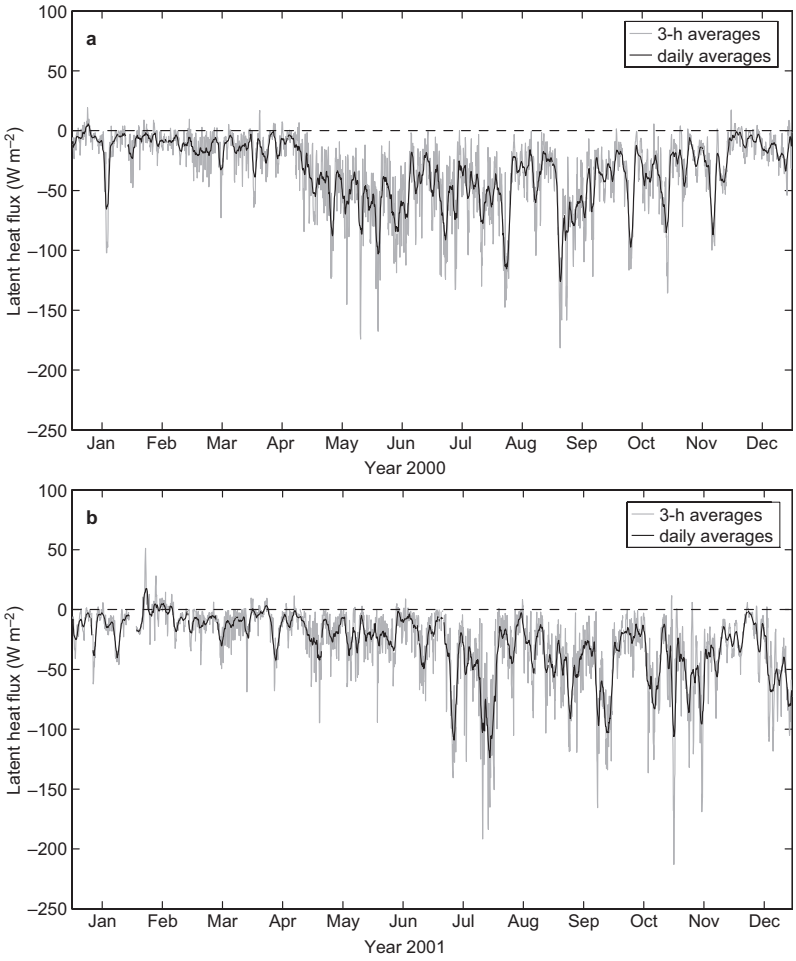

Fig. 5. Latent heat fluxes in (**a**) 2000 and (**b**) 2001.

Heat fluxes from ice growth and melting

The ice-thickness data obtained during the Hanko experiment were collected on a weekly basis. We calculated the latent heat released/used from the ice formation/melting, and the net surface heat fluxes during the same periods (weekly differences) are presented in the previous section.

Here, we compare the latent heat flux released/used by the ice, and the net upper boundary heat fluxes during the ice thickness measurements in 2000 and 2001 (Fig. 9). The difference between them corresponds to the oceanic heat flux from the Santala Bay waterbody to the ice. The curves in Fig. 9 follow each other, and for 2001 they are quite close to each other that indicates the presence of a small oceanic heat flux. In 2000, a large oceanic heat flux at the beginning of the ice season is evident. The surface heat loss was much below the heat release due to ice growth. The difference was up to 50 W m^{-2}, which would be fairly large to represent the oceanic heat flux at the site. At the moment, there is no explanation for this feature; looking at the individual heat flux components (Tables 6 and 7) none seems to be abnormal. At the end of the 2000 ice season, the net surface heat flux was relatively high, more than used for ice melting. This is probably due to the penetration of the solar radiation through the ice sheet. Finally, there seemed to be a delay between the compared fluxes, especially in the middle of the ice season. A temporary storage of heat as sensible heat within the ice sheet, cannot be large enough to explain this delay.

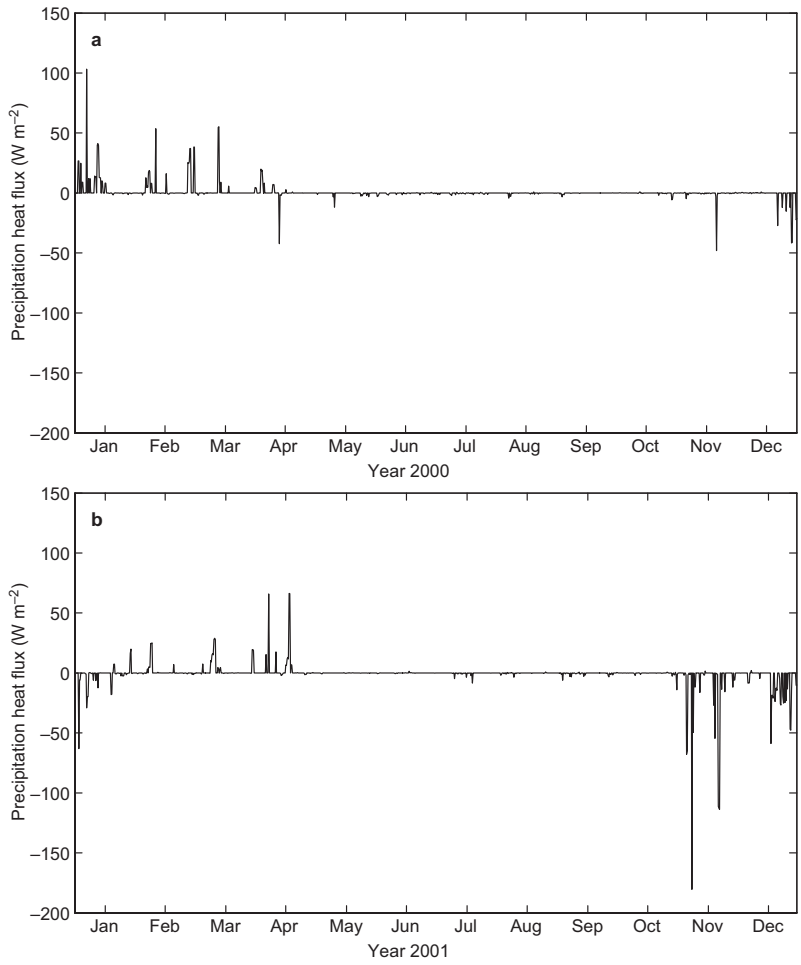

Fig. 6. Heat flux from precipitation in (**a**) 2000 and (**b**) 2001.

Table 4. Sea surface heat balance (W m^{-2}) in Santala Bay in 2000.

	Net solar radiation	Net terrestrial radiation	Sensible heat flux	Latent heat flux	Precipitation heat flux	Net heat flux
January	5	–46	–1	–12	5	–50
February	9	–43	–2	–8	4	–41
March	53	–50	1	–14	2	–10
April	116	–42	1	–16	1	58
May	163	–59	–14	–52	0	38
June	153	–50	–13	–53	0	37
July	114	–42	–9	–52	0	10
August	95	–46	–5	–43	0	0
September	58	–69	–15	–57	0	–82
October	16	–43	–11	–40	0	–78
November	3	–37	–13	–29	–1	–76
December	4	–41	–6	–12	–2	–57
Mean	67	–47	–7	–32	–1	–19

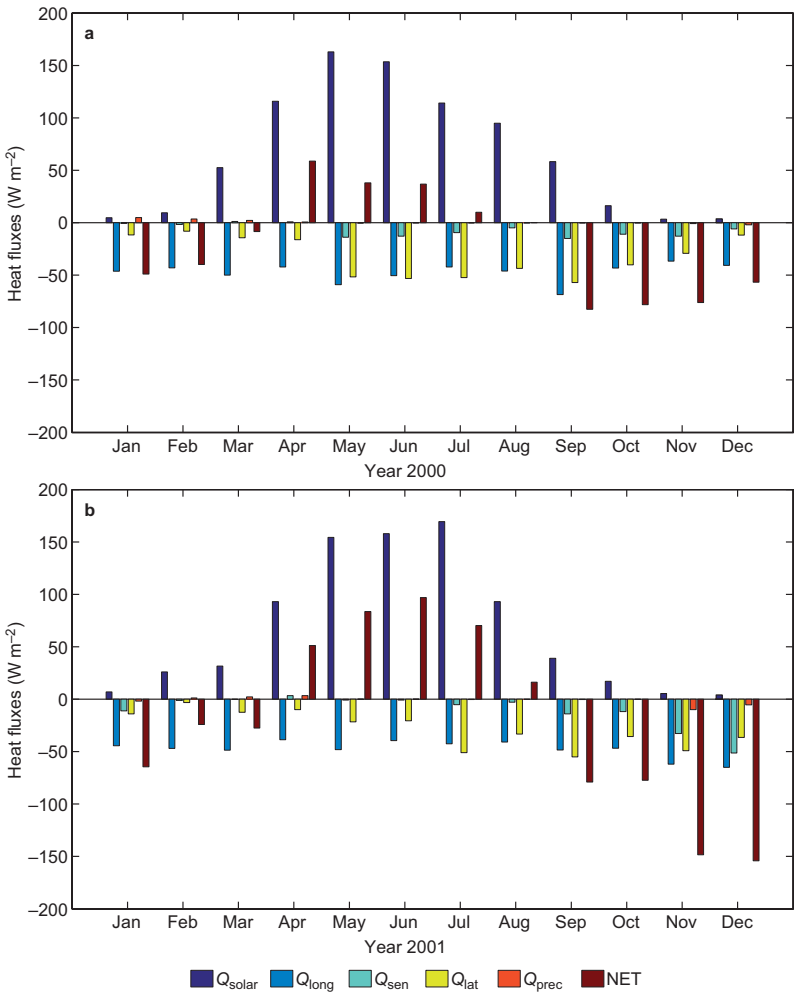

Fig. 7. Monthly averages of the heat flux components for (**a**) 2000 and (**b**) 2001. Q_{solar} = net solar radiation, Q_{long} = net terrestrial radiation, Q_{sen} = sensible heat flux, Q_{lat} = latent heat flux, Q_{prec} = precipitation heat flux, NET = net heat flux.

Table 5. Sea surface heat balance (W m^{-2}) in Santala Bay in 2001.

	Net solar radiation	Net terrestrial radiation	Sensible heat flux	Latent heat flux	Precipitation heat flux	Net heat flux
January	7	−44	−11	−14	−2	−65
February	26	−47	−1	−3	1	−24
March	31	−49	0	−13	2	−28
April	93	−39	3	−10	3	51
May	154	−48	−1	−22	0	84
June	158	−39	−1	−21	0	97
July	169	−43	−5	−51	0	70
August	93	−41	−3	−33	0	16
September	39	−49	−14	−55	0	−79
October	17	−47	−12	−36	0	−77
November	5	−62	−33	−49	−10	−148
December	4	−65	−51	−36	−5	−154
Mean	66	−48	−11	−29	−1	−21

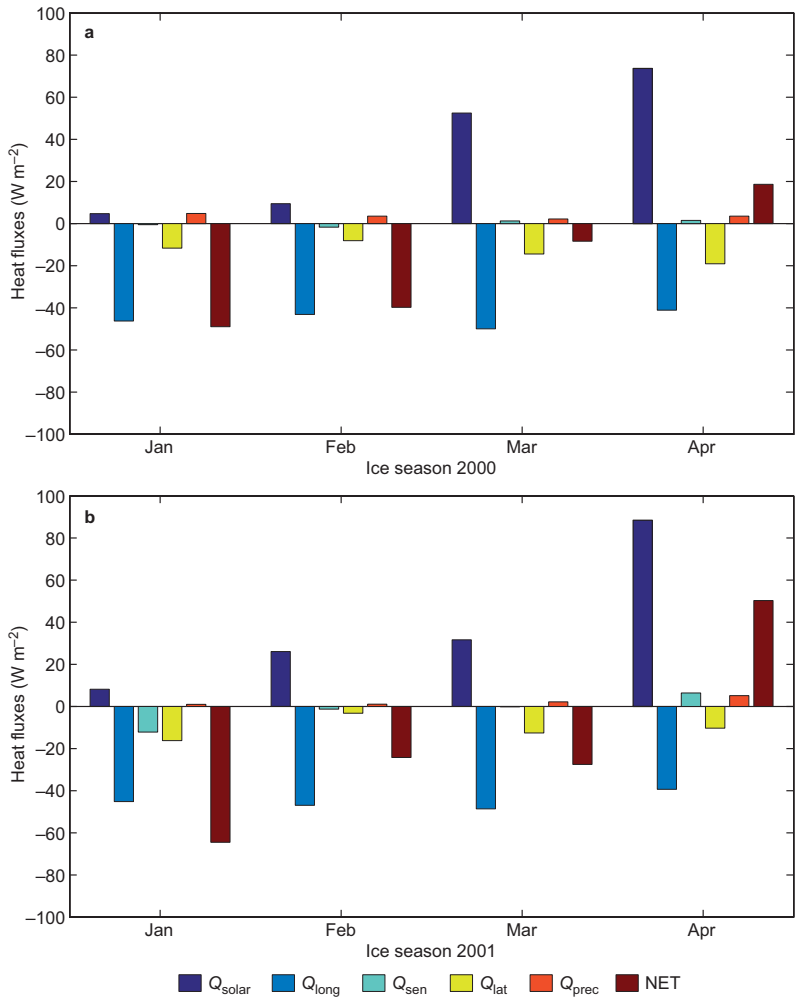

Fig. 8. Monthly averages of the surface heat flux components during the (**a**) 2000 and (**b**) 2001 ice seasons. For sybmol explanations *see* Fig. 7.

Table 6. Radiation components and net radiation balance (W m^{-2}) in Santala Bay in 2000.

	Solar radiation		Terrestrial radiation		Net radiation balance
	Incoming	Outgoing	Incoming	Outgoing	
January	10	–7	255	–302	–44
February	28	–22	260	–303	–37
March	90	–40	254	–304	0
April	130	–14	288	–330	74
May	177	–14	304	–363	104
June	165	–12	330	–380	103
July	123	–9	354	–397	71
August	102	–7	343	–389	49
September	63	–4	308	–376	–9
October	18	–1	318	–362	–27
November	4	0	306	–343	–33
December	4	0	283	–324	–37

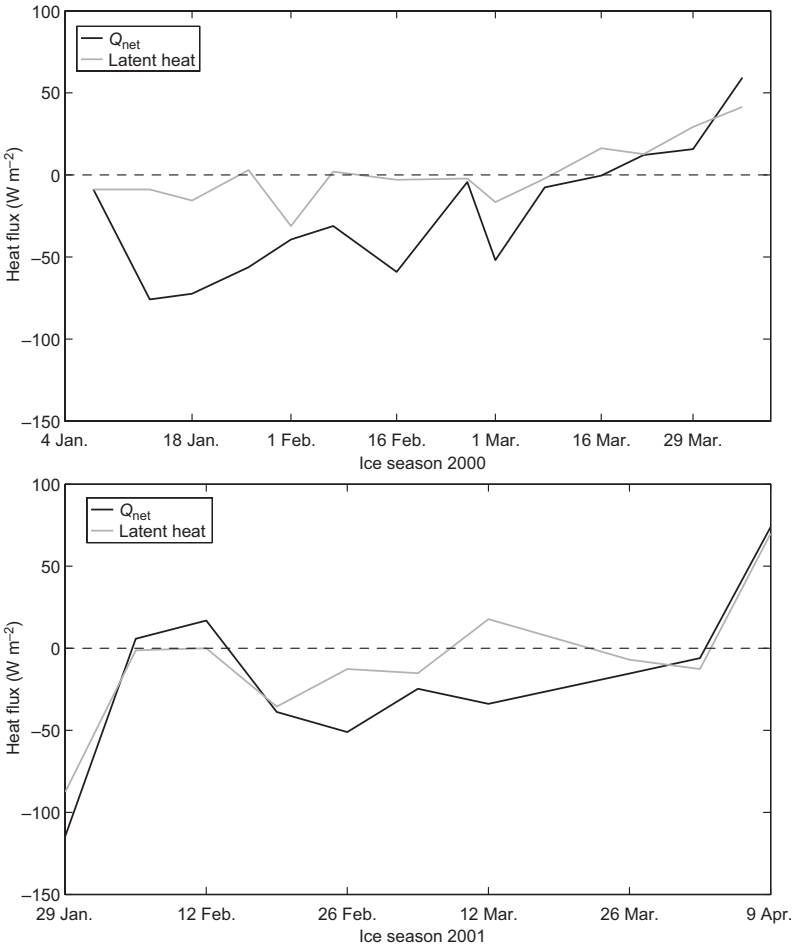

Fig. 9. Comparisons between latent heat released/used from ice thickness measurements and net surface heat fluxes.

Table 7. Radiation components and net radiation balance (W m^{-2}) in Santala Bay in 2001.

	Solar radiation		Terrestrial radiation		Net radiation balance
	Incoming	Outgoing	Incoming	Outgoing	
January	10	–3	269	–314	–38
February	54	–29	232	–279	–22
March	95	–65	245	–294	–19
April	113	–20	286	–324	55
May	167	–12	300	–348	107
June	170	–12	331	–371	118
July	182	–13	366	–408	127
August	100	–7	350	–391	52
September	42	–3	333	–382	–10
October	18	–1	316	–363	–30
November	6	0	270	–332	–56
December	4	0	247	–312	–61

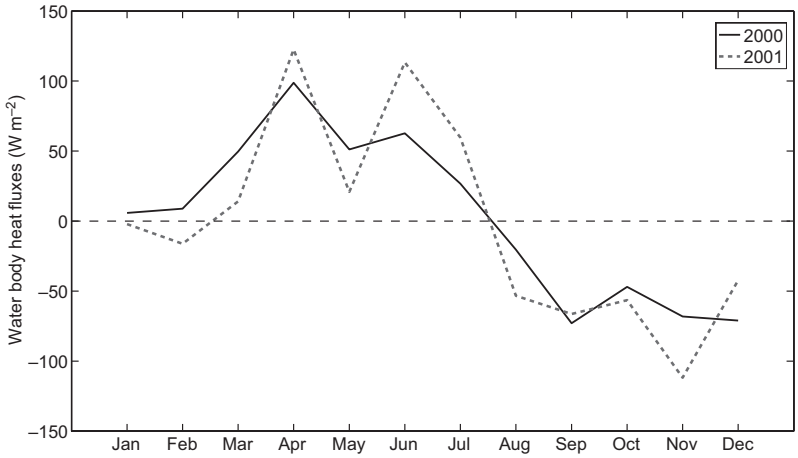

Fig. 10. Heat gain/loss of the Santala Bay waterbody from water temperature differences.

Heat changes in the waterbody

Assuming that Santala Bay is well mixed due to its shallowness, the heat loss/gain of its waterbody due to water temperature changes was estimated as follows (Leppäranta and Myrberg 2009):

$$\Delta Q_w = \frac{\rho_w c_w \Delta T_w H}{\Delta t} \quad (12)$$

where, ΔQ_w is the heat loss/gain of the waterbody, ρ_w is the density of water, c_w is the specific heat of water, H is the depth (here equal to 10 m, and Δt is the time step.

In both years, the waterbody started gaining heat in February–March and started losing heat after July (Fig. 10). The complete heat budget of Santala Bay shows that the local change of heat storage equals the solar and atmospheric surface heat flux and the advective heat flux from the central gulf. The local change consists of temperature changes and phase changes due to freezing and melting.

In both years, monthly averages of the heat gain/loss of the waterbody followed the changes in ice, with a small lag in the bay's response to the surface variations (Fig. 11). The difference between the curves corresponds to advective heat exchange between the central gulf and the site. In both years, there was a strong advection of heat to Santala Bay in autumn, while in summer 2001 the surface heating was strong in Santala Bay resulting in advection of heat out of it.

Ice grows when the air temperature is negative, while at the start of melting the air temperature is about to cross 0 °C (Fig. 12). Even though melting is governed by solar radiation, its starting seems to be closely connected to air temperature. The average air temperature in 2001 was 6.3 °C, 1 °C lower than the average in 2000 (7.4 °C). During the ice seasons in 2000 and 2001, the average air temperatures reached –2.4 °C and –0.7 °C, respectively. Clearly, the winter 2001 was colder and this is reflected in the greater ice thickness.

Discussion

In this study, we presented the annual course of the heat budget in Santala Bay (Gulf of Finland), and attempted to estimate the oceanic heat flux to the ice bottom and the advective heat change between Santala Bay and the central Gulf of Finland.

At the Finnish coast, sea ice occurs every winter, and its influence on the physics and the ecology is significant. The ice acts as an insulator between the ocean and atmosphere and controls the thermodynamics. The thermodynamic processes, analyzed for Santala Bay, run the annual course of sea ice and water temperature in the coastal zone of the Baltic Sea. In winter, solar and terrestrial radiation control the growth and melting of the sea ice. Here, each of the heat exchange components was evaluated for the

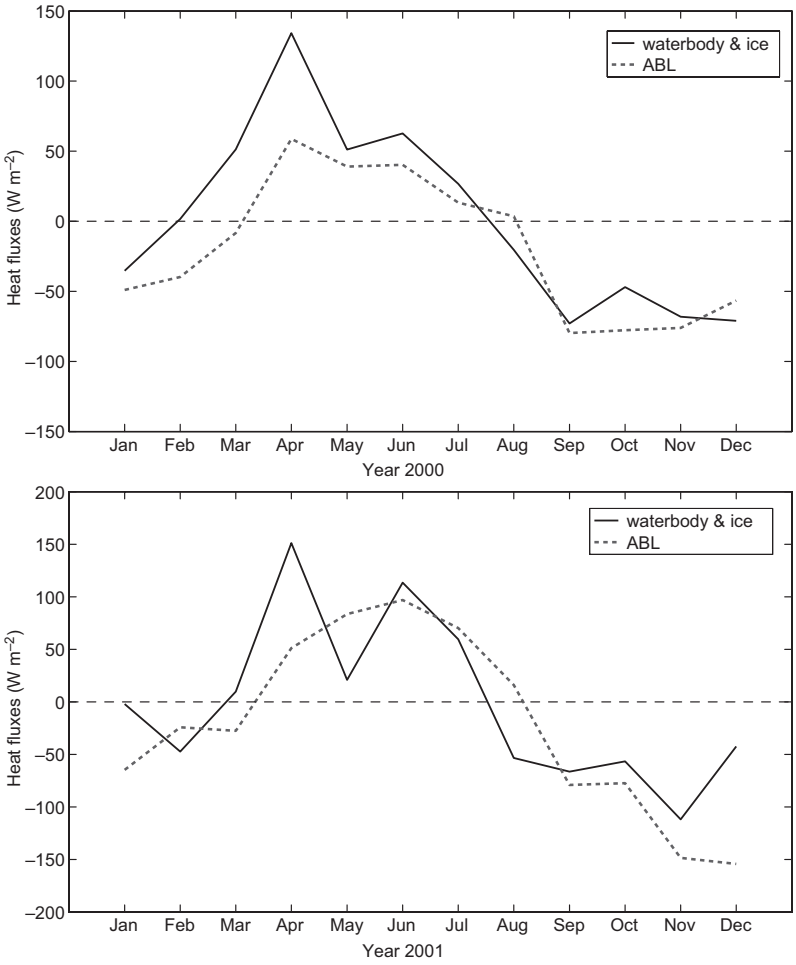

Fig. 11. Monthly averages of heat gain/loss of the waterbody due to water temperature variations added to the latent heat released/absorbed from ice formation/melting, and the net surface heat fluxes (ABL).

years 2000 and 2001 with a 3-hour time-step. This work is the first study of the annual (including the ice season) cycle of the heat budget at Baltic Sea site, based purely on observations. Several heat budget studies were performed with model simulations (e.g., Omstedt 1990), but they are only as good as the models themselves.

A fully open-water annual heat budget was examined by Hankimo (1964) for Finngrundet (Gulf of Bothnia) (for surface heat balance components and with net heat balance *see* Table 8). Due to the ice presence in Santala Bay, and consequently the higher albedo, there are lower values of the solar radiation flux in the ice season. The winter sensible and latent heat fluxes presented in this paper differ from those of Hankimo (1964). The reason is probaby the sites' locations and their proximity to land masses. Hankimo's site was Finngrundet, in the central Gulf of Bothnia, while ours is close to land. Wind speeds are higher, and the difference between air and sea temperatures smaller on high seas as compared with those in coastal areas. The annual averages were similar, but the Santala values are much closer to zero during the ice season. This is reasonable since Santala Bay was ice covered and the sea ice presence can change the air–sea heat and moisture fluxes significantly (Brummer *et al*. 2005). The other heat flux components are within the limits defined by previous research in the Baltic Sea.

The combination of the above reasons resulted in a negative net-heat budget in Santala (~ –20 W m^{-2}) in both years, when Hankimo's was positive (25 W m^{-2}) caused by strong solar heating in summer, presumably due to low

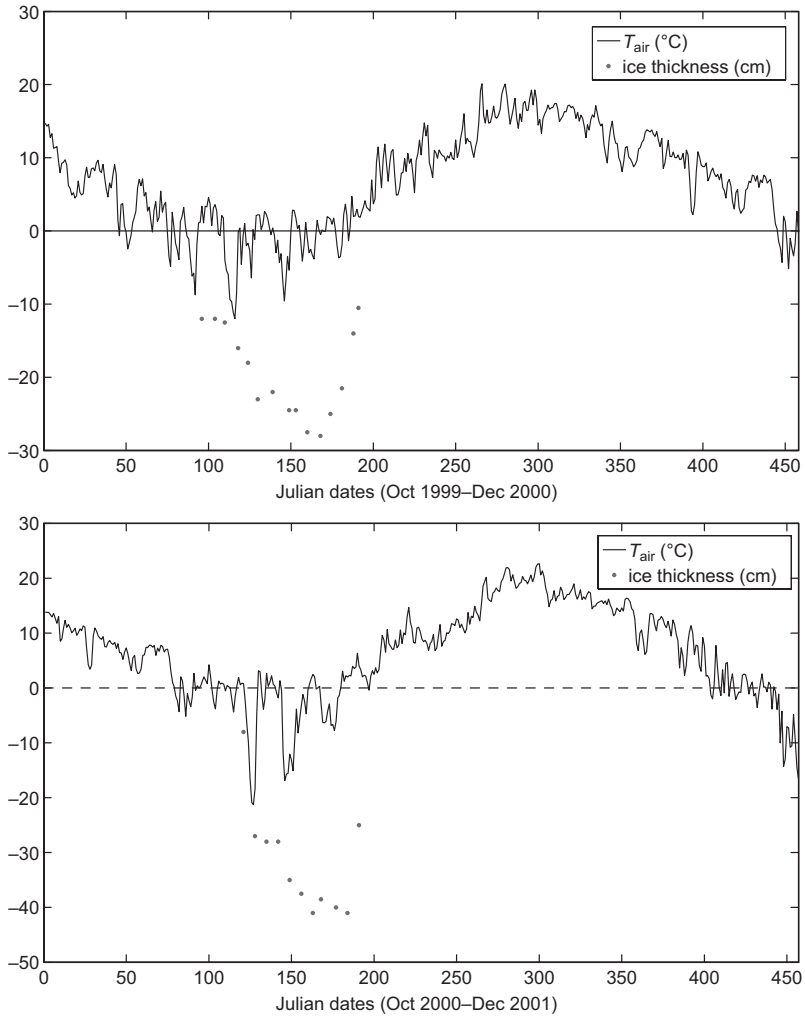

Fig. 12. Daily air temperature and ice thickness variations in two periods.

Table 8. Sea surface heat balance (W m^{-2}) at Finngrundet, south-western Gulf of Bothnia, in March 1961–February 1962 based on observations (data from Hankimo 1964).

	Net solar radiation	Net terrestrial radiation	Sensible heat flux	Latent heat flux	Net heat flux
January	11	–49	–41	–53	–132
February	33	–44	–41	–56	–108
March	91	–56	14	–30	19
April	175	–67	12	–13	107
May	230	–50	17	–1	196
June	295	–52	18	–3	257
July	259	–47	5	–17	200
August	184	–46	5	–46	97
September	113	–53	4	–53	11
October	48	–44	2	–49	–43
November	18	–49	–22	–67	–120
December	8	–54	–58	–81	–186
Mean	122	–51	–7	–39	25

cloudiness. The mean circulation in the Gulf of Bothnia forms a counterclockwise (Leppäranta and Myrberg 2009) gyre so that Finngrundet receives colder water from the north, which likely compensates for the positive surface heat balance. It is important to know the annual net surface heat flux, since it is giving information on advective processes in the water. The annual negative heat balance of Santala Bay was compensated by advection of heat from the Gulf of Finland, while in Hankimo's case there was advection of cold water from the north.

The turbulent heat fluxes in the Baltic Sea simulated by Rutgersson *et al*. (2001) showed similar results to ours. Higher values occurred mainly in autumn. The difference was again during the ice season, when our values were closer to zero due to the ice presence. Rutgersson *et al*. (2001) noticed overestimation of the turbulent fluxes in two model simulations (HIRLAM and PROBE-Baltic). Our annual averages for the heat flux components are within the limits of past model studies and observations in the Baltic Sea (Omstedt *et al*. 2000, Meier and Döscher 2002, Niros *et al*. 2002, Döscher and Meier 2004).

This is the first time that the latent heat fluxes from ice growth and melting and the net surface heat flux are being compared. The patterns are similar and the differences can be, at least partly, attributed to the oceanic heat flux and to the solar penetration through the sea ice, especially at the end of the ice season. This comparison can be also used as a measure of method inaccuracies.

Estimation of the heat budget includes in general several critical parameters. For solar radiation it is the albedo of snow and ice, however in this study it was directly measured during the ice season. Longwave radiation coming from the atmosphere is the most difficult term. Here, it was parameterized in terms of cloudiness and humidity, and the numerical coefficients were taken from the earlier Baltic Sea studies. Since the values of cloudiness were taken from the Russarö weather station further offshore from Santala Bay, the atmospheric radiation fluxes obtained here are somewhat overestimated in spring and summer and underestimated in autumn.

Conclusions

On the whole, the heat exchanges between the surface and the atmosphere follow the normal pattern. The surface heat flux is mainly controlled by the radiation balance, solar radiation heating in spring and summer and the longwave radiation cooling in autumn and winter. Turbulent heat fluxes were comparable to the longwave radiation losses in autumn, and on average the magnitude of latent heat flux was higher than that of sensible heat flux. Heat fluxes connected with precipitation were substantial when phase changes were involved, but remained small in the monthly averages.

The solar radiation was on average 67 W m^{-2} in 2000 and 66 W m^{-2} in 2001, with a maximum 3-hour value of 705 W m^{-2}. In both years, the net longwave terrestrial radiation was mostly negative with the same average value of –50 W m^{-2}. The minimum 3-hour value –140 W m^{-2} was measured in 2001. The lowest values were due to high differences between the atmosphere and surface temperatures. The monthly average sensible heat fluxes were low in comparison with the radiation terms. However, their fluctuation was considerable: minimum 3-hour values reached –228 W m^{-2} (year 2001), and maximum 3-hour values 77 W m^{-2} (year 2000). The latent heat flux had a greater effect on the heat budget than the sensible heat flux with negative values, except occasionally in winter, due to sublimation of moisture on the ice surface. The average values were –30 W m^{-2} for both years, and the minimum 3-hour values –203 W m^{-2} in 2001.

The closure of the surface heat flux was examined based on local changes at the site. In the ice season, nonzero surface flux results in ice growth or melting, and the residual then equals the oceanic heat flux from the water to the ice. The comparison between changes of the ice thickness and the net surface heat fluxes showed similar patterns in both years but the fit was much better in 2001. The difference is due to the oceanic heat flux and estimation errors. In January–February 2000 this difference was about –50 W m^{-2}, which would be an unrealistically large level of oceanic heat flux at the site. The reason for this is not clear. On the whole, it seems that

sea ice can be used as a measure for controlling the net surface heat fluxes. The residual from the changes in the local heat storage, ice and water together, and surface flux provide an estimate for the advective heat exchange between the coastal site and the central gulf. The result showed that there was a positive average heating of the coastal site, which dominates in autumn.

Acknowledgements: We thank the personnel of Tvärminne Zoological Station for their help in organizing the fieldwork and providing laboratory facilities. Professor Marko Reinikainen, director of the Tvärminne Zoological Station provided us with the surface temperature data during the open water season. Ioanna Merkouriadi has been supported by Vilho, the Yrjö and Kalle Väisälä Foundation of the Finnish Academy of Sciences and Letters, which is gratefully acknowledged.

References

Andreas E. 1987. A theory for the scalar roughness and the scalar transfer coefficients over snow and sea ice. *Boundary-Layer Meteorology* 38: 159–184.

Arst H., Erm A., Leppäranta M. & Reinart A. 2006. Radiative characteristics of ice-covered fresh- and brackish-water bodies. *Proc. Estonian Acad. Sci. Geol.* 55: 3–23.

Brummer B., Kirchgäßner A. & Müller G. 2005. The atmospheric boundary layer over Baltic Sea ice. *Boundary-Layer Meteorology* 117: 91–109.

Döscher R. & Meier M. 2004. Simulated sea surface temperature and heat fluxes in different climates of the Baltic Sea. *Royal Swedish Academy of Sciences* 33: 242–248.

Ehn J., Granskog M.A., Reinart A. & Erm A. 2004. Optical properties of melting landfast sea ice and underlying seawater in Santala Bay, Gulf of Finland. *Journal of Geophysical Research* 109, C09003, doi:10.1029/2003JC002042.

Garratt J.R. 1992. *The atmospheric boundary layer*. Cambridge University Press, Melbourn.

Granskog M., Leppäranta M., Ehn J., Kawamura T. & Shirasawa K. 2004. Seasonal development of the properties and composition of landfast sea ice in the Gulf of Finland, the Baltic Sea. *Journal of Geophysical Research* 109, C02020, doi:10.1029/2003JC001874.

Hankimo J. 1964. Some computations of the energy exchange between the sea and the atmosphere in the Baltic area. *Ilmatieteellisen Keskuslaitoksen Toimituksia* 57: 1–26.

Holtslag A.A.M. & De Bruin H.A.R. 1988. Applied modeling of the nighttime surface energy balance over land. *Journal of Applied Meteorology* 27: 689–704.

Högström U. 1988. Non-dimensional wind and temperature profiles in the atmospheric surface layer: a re-evaluation. *Boundary-Layer Meteorology* 42: 55–78.

Iqbal M. 1983: *An introduction to solar radiation*. Academic Press, Toronto.

Kawamura T., Shirasawa K., Ishikawa N., Lindfors A., Rasmus K., Ehn J., Leppäranta M., Martma T. & Vaikmäe R. 2001. A time series of the sea ice structure in the Baltic Sea. *Annals of Glaciology* 33: 1–4.

Kawamura T., Granskog M.A., Lindfors A., Ehn J., Martma T., Vaikmäe R., Ishikawa N., Shirasawa K. & Leppäranta M. 2002. Study of brackish ice in the Gulf of Finland — effect of salt on sea ice structure. In: *Proc. 16th IAHR Ice Symposium* vol. 2, Dunedin, New Zealand, pp. 165–171.

Launiainen J. & Saarinen J. 1982. Examples of comparison of wind and air–sea interaction characteristics on the open sea and in the coastal area of the Gulf of Finland. *Geophysica* 19: 33–46.

Launiainen J. & Vihma T. 1990. Derivation of turbulent surface fluxes — an iterative flux-profile method allowing arbitrary observing heights. *Environmental Software* 5: 113–124.

Launiainen J. & Vihma T. 2001. Turbulent surface fluxes and air–sea coupling in the Baltic Air–Sea–Ice study (BASIS). *Annals of Glaciology* 33: 237–242.

Lumb F.E. 1963. The influence of cloud on hourly amounts of total solar radiation at the sea surface. *Quarterly Journal of the Royal Meteorological Society* 90: 43–56.

Leppäranta M. & Myrberg K. 2009. *Physical oceanography of the Baltic Sea*. Springer-Praxis, Heidelberg.

Meier M. & Döscher R. 2002. Simulated water and heat cycles of the Baltic Sea using a 3D coupled atmosphere-ice-ocean model. *Boreal Environmental Research* 7: 327–334.

Niros A., Vihma T. & Launiainen J. 2002. Marine meteorological conditions and air–sea exchange processes over the northern Baltic Sea in the 1990s. *Geophysica* 38: 59–87.

Obukhov A.M. 1981. Turbulence in an atmosphere with a non-uniform temperature. *Boundary-Layer Meteorology* 2: 7–29.

Omstedt A. 1990. Modelling the Baltic Sea as thirteen subbasins with vertical resolution. *Tellus* 42A: 286–301.

Omstedt A. & Rutgersson A. 2000. Closing the water and heat cycles of the Baltic Sea. *Meteorologische Zeitschrift* 9: 57–64.

Reinart A. & Arst H. 1998. Relation between underwater irradiance in dependence on water transparency at different depths in the water bodies. *Journal of Geophysical Research* 103: 7749–7752.

Rutgersson A., Smedman A.S. & Omstedt A. 2001. Measured and simulated latent and sensible heat fluxes at two marine sites in the Baltic Sea. *Boundary-Layer Meteorology* 99: 53–84.

Saloranta T. 2000. Modelling the evolution of snow, snow-ice and ice in the Baltic Sea. *Tellus* 52A: 93–108.

Seinä A. & Peltola J. 1991. Duration of the ice season and statistics of fast ice thickness along the Finnish coast. *Finnish Marine Research* 258: 1–46.

Shirasawa K., Leppäranta M., Kawamura T., Ishikawa M. & Takatsuka T. 2006. Measurements and modelling of the water — ice heat flux in natural waters. In: *Proceedings of the 18th IAHR International Symposium on Ice*,

Hokkaido University, Sapporo, Japan, pp. 85–91.

Weeks W.F. 1998. Growth conditions and the structure and properties of sea ice. In: Leppäranta M. (ed.), *Physics of ice-covered seas*, 1: 25–104. Helsinki University Press.

Zillman J.W. 1972. *A study of some aspects of the radiation and heat budgets of southern hemisphere oceans*. Report 26, Department of International Meteorological Studies, Bureau of Meteorology, Canberra.